CrossMark

ORIGINAL ARTICLE

Seed development of *Jatropha curcas* L. (Euphorbiaceae): integrating anatomical, ultrastructural and molecular studies

Emanoella L. Soares[1] · Magda L. B. Lima[1] · José R. S. Nascimento[1] ·
Arlete A. Soares[2] · Ítalo A. C. Coutinho[2] · Francisco A. P. Campos[1] ⓘ

Abstract

Key message **This work provides a detailed histological analysis of the development of *Jatropha curcas* seeds, together with an assessment of the role of programmed cell death in this process.**

Abstract Seeds of *Jatropha curcas* are a potential source of raw material for the production of biodiesel, but very little is known about how the architecture of the seeds is shaped by the coordinated development of the embryo, endosperm and maternal tissues, namely integuments and nucellus. This study used standard anatomical and ultrastructural techniques to evaluate seed development and programmed cell death (PCD) in the inner integument was monitored by qPCR. In these studies, we found that the embryo sac formation is of the *Polygonum* type. We also found that embryogenesis is a slow process and the embryo is nourished by the suspensor at earlier stages and by nutrients remobilized from the lysis of the inner integument at later stages. Two types of programmed cell death contribute to the differentiation of the inner integument that begins at early stages of seed development. In addition, the mature embryo presents features of adaptation to dry environments such as the presence of four seminal roots, water absorbing stomata in the root zone and already differentiated protoxylem elements. The findings in this study fill in gaps related to the ontogeny of *J. curcas* seed development and provide novel insights regarding the types of PCD occurring in the inner integument.

Introduction

Jatropha curcas L. seeds have been proposed as a source of raw material for the production of biodiesel, but the tapping of this potential is hampered by the lack of basic knowledge regarding the developmental biology of these seeds (Mardhiah et al. 2017). For example, very little is known on how the architecture of *J. curcas* seeds is shaped by the coordinated development of the embryo, endosperm and maternal tissues. The lack of this knowledge limits our understanding on the relative contribution of these structures as nutrient reserves and the precise role of the integument as a conduit of carbon and nitrogen from source organs to the growing embryo and endosperm, and as reservoir of nutrients in itself.

The availability of a draft genome of *J. curcas* (Sato et al. 2011; Hirakawa et al. 2012) and of a flurry of transcriptomic data (Costa et al. 2010; Natarajan et al. 2010; King et al. 2011; Rocha et al. 2013; Laosatit et al. 2016) is enabling studies geared towards establishing the proteome changes associated with seed development both in maternal and zygotic tissues as well as the establishment of expression patterns of genes associated with the synthesis of fatty acids and phorbol esters in the seeds. However, because the precise temporal and spatial patterns of formation of the integuments, endosperm and embryo are lacking, there are uncertain assignments of biological

✉ Francisco A. P. Campos
    bioplant@ufc.br

1   Departamento de Bioquímica e Biologia Molecular,
    Universidade Federal do Ceará, Fortaleza, CE, Brazil

2   Departamento de Biologia, Universidade Federal do Ceará,
    Fortaleza, CE, Brazil

⚫ Springer

meaning associated with the proteomic and transcriptomic data. This happens because generally tissue samples used in these studies are obtained disregarding either the developmental stage of the seeds or the proper separation of the pertinent seed tissues (Natarajan and Parani 2011; Xu et al. 2011; Liu et al. 2013).

As these tissues share many metabolic and biosynthetic pathways, the expression pattern of a transcript or protein will not be informative if their tissue source is not precisely known. For example, many of the peptidases which are known to be involved in the maturation of seed reserve proteins during the filling stage of the endosperm of many Euphorbiaceae seeds, have also a role during the programmed cell death (PCD) of the integuments (Soares et al. 2014; Shah et al. 2015).

Although there are some reports dealing with the anatomy of *J. curcas* seeds (Singh 1970; Rocha et al. 2013; Soares et al. 2014; Shah et al. 2015), data about embryo sac formation, embryogenesis, endosperm development, seed coat differentiation and adaptive features to arid or semi-arid environments of the mature embryo are still missing. Here we provide such missing data and a detailed ultrastructural analysis that illuminate the types of programmed cell death taking place at the developing seed coat.

Materials and methods

Plant material and anatomical analysis

Jatropha curcas plants used for all analysis were grown as previously described (Soares et al. 2014; Shah et al. 2015). Floral buds were collected according to their lengths (1, 2, 3 and 4 mm). Developing seeds were collected 1, 2, 3, 5, 7, 10, 15, 20, 22, 25, 30 and 35 days after pollination (DAP). Such seeds were collected from hand-pollinated flowers that had been restricted from pollinators. Flowers were kept away from pollinators using tulle bags.

Histological analysis of the buds and developing seeds were performed as previously described (Soares et al. 2014; Shah et al. 2015). Cross and longitudinal sections about 3–5 μm thick were made in an automated rotary microtome (Leica Biosystems, Nussloch, Germany) and stained with 0.5% toluidine blue followed by 0.5% basic fuchsine (Junqueira 1990).

Transmission electron microscopy (TEM)

Transmission electron microscopy analysis of the mesophyll of the inner integument from ovule and developing seeds at 5, 10 and 25 DAP was based on the protocol of Shah et al. (2016). All samples were 1 mm² hand-cut with a razor blade. Seeds at 10 and 25 DAP were divided in two

regions for the analysis, i.e. proximal and distal region. The former corresponded to the innermost layers of the inner integument close to the central cavity versus the outermost layers of the mesophyll of the inner integument close to the endotegmen.

Scanning electron microscopy (SEM)

Root apexes from mature embryo of *J. curcas* were isolated, immediately fixed in Karnovsky solution (Karnovsky 1965) for 24 h and rinsed three times in 0.1 M phosphate buffer solution at pH 7.2. Samples were then post-fixed with 1% osmium tetroxide for 1 h, rinsed five times with distilled water, dehydrated through a graded ethanol series from 30 to 100% (15 min to each step), dried at critical point with CO_2 and sputter coated with gold (Emitech model K 550, Sussex, England) for analysis with a SEM (VEGA3 TESCAN, Kohoutovice, Czech republic) operating at 15 kV.

Confocal microscopy

Apical roots from whole mature embryos were submersed in the apoplastic tracer Lucifer Yellow (Oparka and Prior 1988) for 1 h and rinsed with distilled water. Hand-sections of the root apexes made with the aid of a razor blade were then mounted in glycerin:water (1:1) and observed in a confocal microscope (Zeiss 710, Oberkochen, Germany) with DAPI UV filter (Axiophot model). Emissions were collected between 550 and 600 nm.

Gene expression analysis

Gene expression analysis followed Soares et al. (2014) modified. Total RNA of the inner integument from ovule and developing seeds at 5 and 10 DAP was individually isolated from 100 mg of tissue using the Plant RNA Purification Reagent (Invitrogen, CA, USA). Quantitative reverse transcription PCR (RT-qPCR) was carried out using the BRYT Green GoTaq©qPCR Master Mix (PROMEGA, WI, USA). Reactions were carried out with 20 ng of cDNA and 200 nM of each primer in a final volume of 20 μL. Specific primer sequences for KDEL-tailed cysteine peptidase (Jcr4S00024.130); serine peptidase (Jcr4S01605.60) and subtilisin (Jcr4S01323.10) were manufactured according to Soares et al. (2014). Data normalization was performed with glyceraldehyde-3-phosphate dehydrogenase, elongation factor 1 alpha, ubiquitin carrier protein and protein phosphatase 2 (Rocha et al. 2013; Soares et al. 2014). The gene relative expression was done in relation to the ovule (calibrator). The experimental design was comprised of two biological replicates per sample, each one with three reverse transcriptions (RT) in

triplicate ($n = 9$). The $2^{-\Delta\Delta C_\mathrm{T}}$ method (Livak and Sch-mittgen 2001) was used for the analysis of relative expression.

Results

Ovule structure

The ovule of *J. curcas is* anatropous, bitegmic with exo- and endostome making up the micropyle, crassinucellar, and fills up nearly all the locule (Fig. 1A). The nucellus develops faster than the two integuments and, therefore, is projected out of the micropyle, up to the obturator, forming a nucellar beak (Fig. 1A). The funiculus connects the placenta to the outer integument; the raphe is adjacent to the outer integument; and the chalaza is opposite to the micropyle (Fig. 1B). The vascular tissue branches from the chalaza into the inner integument (Fig. 1B). Over the micropyle, similar to a hood on top of the nucellar beak, placental outgrowths form the obturator (Fig. 1A). The obturator is made up of cells with densely stained cyto-plasm, nucleus mostly central and apical vacuome. A hypostasis with composing cells accumulating phenolic compounds and a caruncle are also observed (Fig. 1B).

The formation of the embryo sac is of the *Polygonum*-type. In ~ 1 mm-length flower buds, the archesporial cell (Fig. 1C, arrow) are distinguished from the other nucellar cells due to its large size, densely stained cytoplasm and with the surrounding large nucleus with conspicuous nucleolus (Fig. 1C). The development of the embryo sac was as observed in 2–4 mm-length flower buds (Fig. 1D–I).

The binuclear embryo sac observed in 2 mm flower buds displayed the central cell less expanded (Fig. 1D) than in 2.5 mm (Fig. 1E). The egg cell had densely stained cytoplasm around the nucleus and well-developed vac-uome in ~ 3 mm flower buds (Fig. 1F, G). In 3.5 mm flower buds, the synergids are next to the egg cell (Fig. 1G)
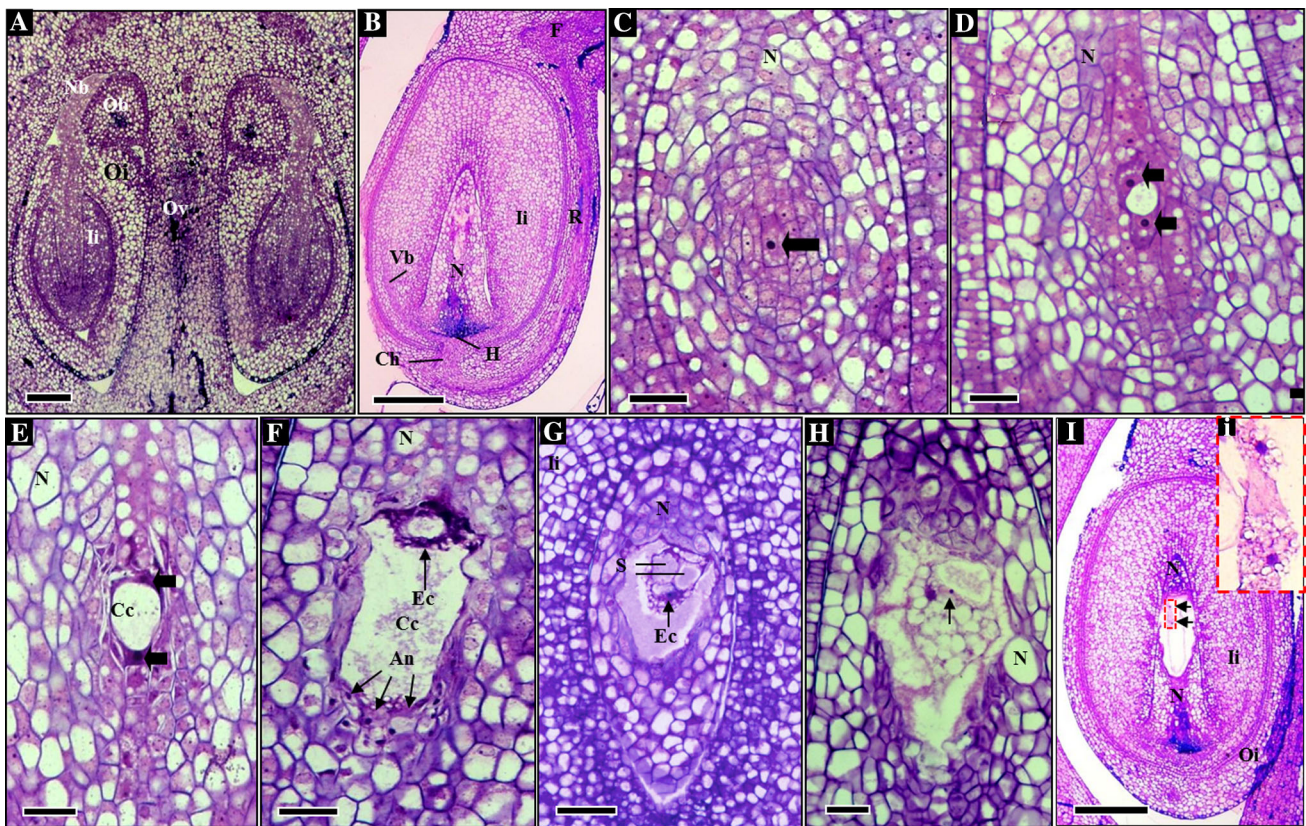

Fig. 1 Ovule anatomy and embryo sac development of *J. curcas* under light microscopy as observed in longitudinal sections of floral buds of 1.0 mm and mature ovule before pollination (**A**, **B**), floral buds of 1.0 mm (**C**), 2.0 mm (**D**), 2.5 mm (**E**), 3.0 mm (**F**), 3.5 mm (**G**) and 4.0 mm (**H**) length. **A** Synchronous development of two ovules. **B** Fully differentiated ovule. **C** Archesporial cell (*arrow*). **D**, **E** Binucleate embryo sac (*arrows*). **F** Embryo sac with antipodal and egg cells. **G** Synergid and egg cells. **H** One polar nuclei (*arrow*) of a mature ovule before pollination. **I** Developing seed at 5 days after pollination showing the endosperm free nuclei (*arrows*) and the expanded central cavity. Note detail of the endosperm free nuclei (*i*). *An* antipodal cell, *Cc* central cavity, *Ch* chalaza, *Ec* egg cell, *F* funiculus, *H* hypostasis, *Ii* inner integument, *N* nucellus, *Nb* nucellar beak, *Ob* obturator, *Oi* outer integument, *Ov* ovary, *R* raphe, *S* synergid cells, *Vb* vascular bundle. *Bars* 20 µm (**A**), 500 µm (**B**), 20 µm (**C**, **D**, **F**, **H**), 50 µm (**E**), 500 µm (**G**) and 20 µm (**I**)

while the three antipodals are in the chalazal side (Fig. 1F). In non-pollinated open flowers, the central cell of the embryo sac has the polar nuclei surrounded by cytoplasm (Fig. 1H). The embryo sac is sunk in the nucellus and placed several layers below the nucellar epidermis due to the parietal cell division of the nucellus itself.

Development of the embryo

Twenty-four hours after pollination we observed the consumption of the middle portion of the nucellus, enlargement of the central cavity of the embryo sac and the beginning of the formation of the nuclear endosperm with free nuclei which appeared at the middle area of the central cavity (Fig. 1I, i). The zygote was formed approximately 48 h after pollination (Fig. 2a), but its first division, which originates the basal and apical cells, was only observed at 10 DAP (Fig. 2b). The pyriform-shaped pre-embryo with a four-celled suspensor was observed at 15 DAP (Fig. 2c). Successive nuclear divisions of the coenocytic endosperm continued up to the early globular stage of the embryo (Fig. 2a–d). At this point, the free nuclei were placed adjacent to the inner integument. Afterwards, only remnants of the nucellus were observed in the micropyle area (i.e. where the embryo stayed attached) and near the chalazal area. Embryos at the globular and heart stages were found 22 DAP (Fig. 2d) and 25 DAP (Fig. 2e),

respectively. In both stages, the embryos were attached to the remnants of the nucellus by the suspensor. At the heart stage, the endosperm surrounding the embryo had already begun the cellularization process (Fig. 2e–g). Endosperm cellularization started at the micropylar area close to the embryo (Fig. 2e, f) and then continued towards the chalazal area, and eventually towards the central cavity. The cellularization of the endosperm is marked by the formation of alveoli in which successive nuclear divisions and formation of new periclinal cell walls gave rise to new layers of cells and alveoli (Fig. 2g). The alveolation as well as the concomitant storage of reserves by the newly formed cells continued until the vacuole of the central cavity was completely filled up with newly formed endosperm cells.

At the early cotyledonal stage the embryo remained attached to the collapsed remnants of the nucellus by the suspensor (Fig. 2h). As the development proceeded, the central cavity continued enlarging. At this stage the nucellus was completely consumed and the suspensor was no longer present. The mature embryo with all meristematic zones developed (i.e. protoderm, ground meristem, procambium, shoot and root meristem) after 35 DAP (Fig. 2i). At this stage, the ground meristem cells were rich in storage reserves.

Several open stomata (Fig. 3a, b) were found on the radicle, including the seminal roots in the mature embryo. Absorption of the apoplastic tracer Lucifer Yellow by such stomata and also by protodermal cells was demonstrated (Fig. 3c). Further,
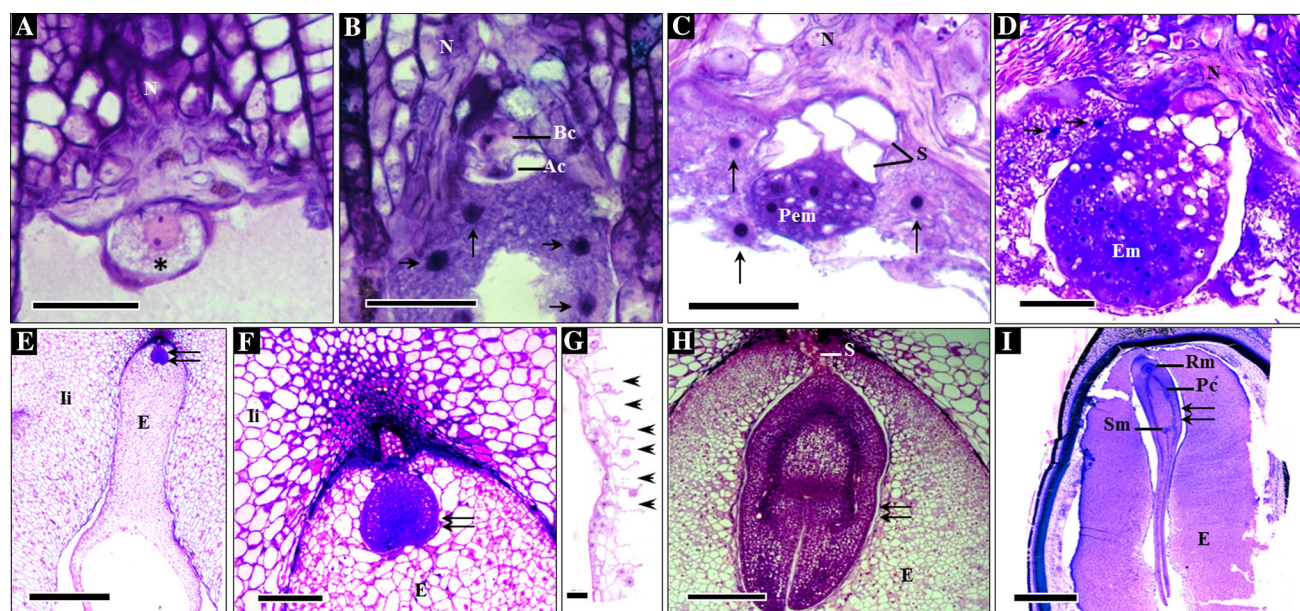

Fig. 2 Embryogenesis of *J. curcas* under light microscopy as observed in longitudinal section seeds at 2 (**a**), 10 (**b**), 15 (**c**), 22 (**d**), 25 (**e, g**), 30 and 35 (**i**) days after pollination. **a** Zygote (*asterisk*). **b** First division of the zygote and free nuclei of the endosperm. **c** Proembryo and free nuclei of the endosperm (*arrow*). **d** Globular embryo and free nuclei of the endosperm (*arrow*). **e–g** Heart-shaped embryo (*double arrow*) and the cellularization of the endosperm with developing alveoli (*arrowhead*). **h** Early cotyledonal embryo (*double arrow*). **i** Late cotyledonal embryo (*double arrow*). *Ac* apical cell, *Bc* basal cell, *E* endosperm, *Em* embryo, *Ii* inner integument, *N* nucellus, *Pc* procambium, *Pem* proembryo, *Rm* root meristem, *S* suspensor, *Sm* shoot meristem. *Bars* 30 μm (**a–d**), 200 μm (**e**), 2 mm (**f, h, i**) and 50 μm (**g**)
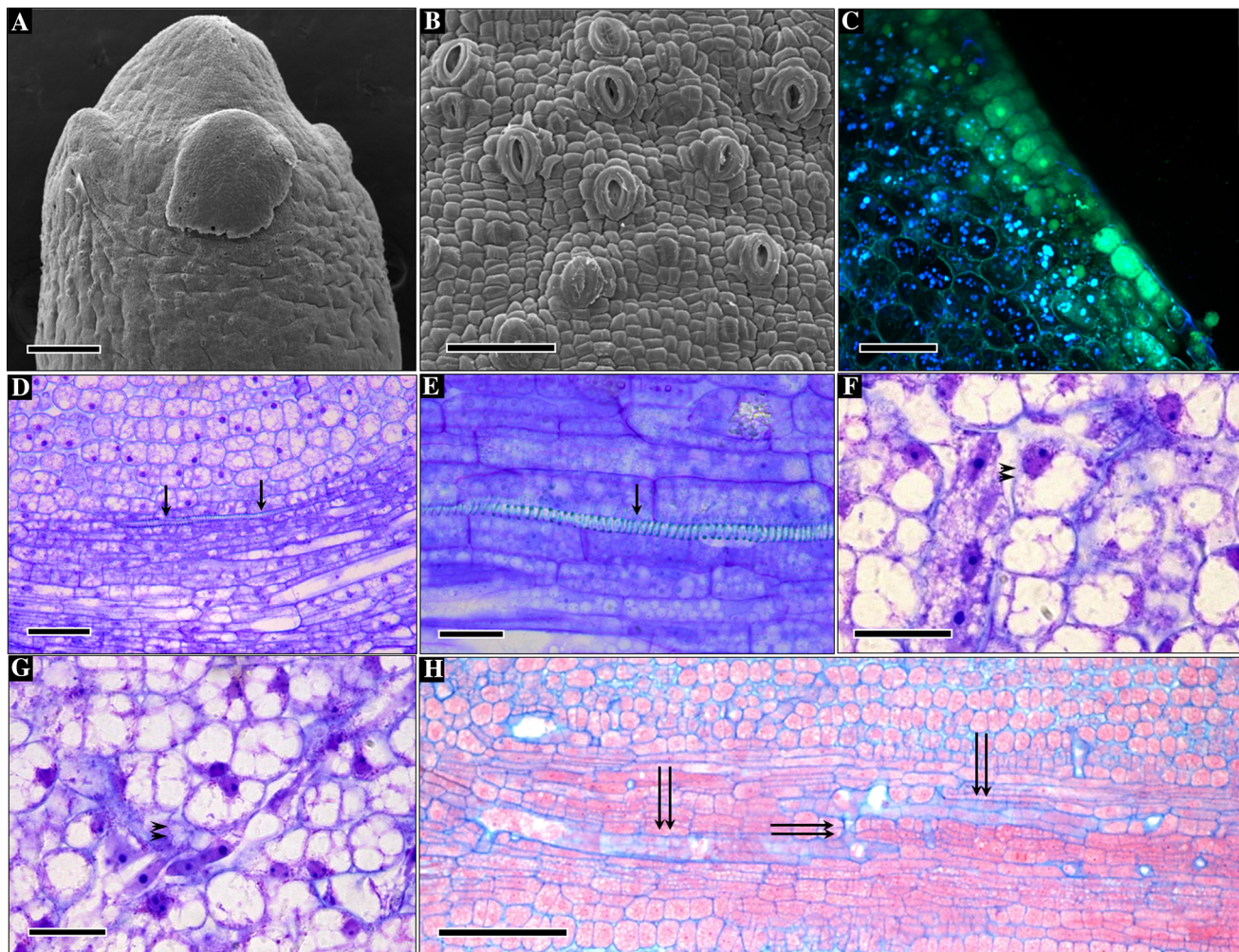
Fig. 3 Mature embryo of *J. curcas* under scanning electron (**a**, **b**), confocal (**c**) and light (**d–i**) microscopy. **a** Root apex of the embryo showing seminal roots. **b** Stomata at the seminal root zone. **c** Water absorption demonstrated by the apoplastic tracer Lucifer Yellow (*yellow-green* fluorescence). **d**, **e** Differentiated protoxylem elements (*arrows*). **f**, **g** Laticifers undergoing differentiation. Note the breakdown of the adjoining cell walls (*arrowhead*) and laticifers with coenocytic nuclei. **h** Anastomosing laticifers (*double arrow*). *Bars* 250 μm (**a**), 50 μm (**b**, **d**), 40 μm (**c**), 20 μm (**e–g**) and 100 μm (**h**) (color figure online)

few protoxylem elements with annular thickenings of the wall were already differentiated (Fig. 3d, e). Laticifers undergoing differentiation were also commonly found (Fig. 3f–h), in which the cells were actively dividing, but the cell wall between the mother and daughter cells was quickly broken down and absorbed (Fig. 3f, g). Connections between parallel rows of laticifers were also observed (Fig. 3h).

The mature endosperm, with cells storing reserves, surrounded the embryo and filled up most of the mature seed (Fig. 2i). Remnants of cell lysis from a few layers of endosperm close to the embryo were observed (Fig. 2i).

Differentiation and ultrastructure of the seed coat

In the non-fertilized ovule, the cells from both integuments layers are similar, but the inner integument is made up of ~20 cell layers, while the outer integument has fewer layers (~10 cell layers) at the raphe area and ~5 cell layers on the opposite side (Figs. 1G, 4a). Both integuments have single-layered inner and outer epidermis composed of thin walled cells with densely stained cytoplasm (Fig. 4a). The mesophyll cells of the integuments are vacuolated and both nuclei and cytoplasm are peripheral, near the cell wall. However, the layers of mesophyll cells of the inner integument next to the inner epidermis of such integument show densely stained cytoplasm and cell divisions (Fig. 4b). Ultrastructural analyses of the mesophyll cells of the inner integument showed several plastids, mitochondrion and a large central vacuole (Fig. 4c).

Five DAP (Fig. 4d), although cell divisions were still taking place, we observed the rupture of the tonoplast (Fig. 4e) and the presence of endoplasmic reticulum
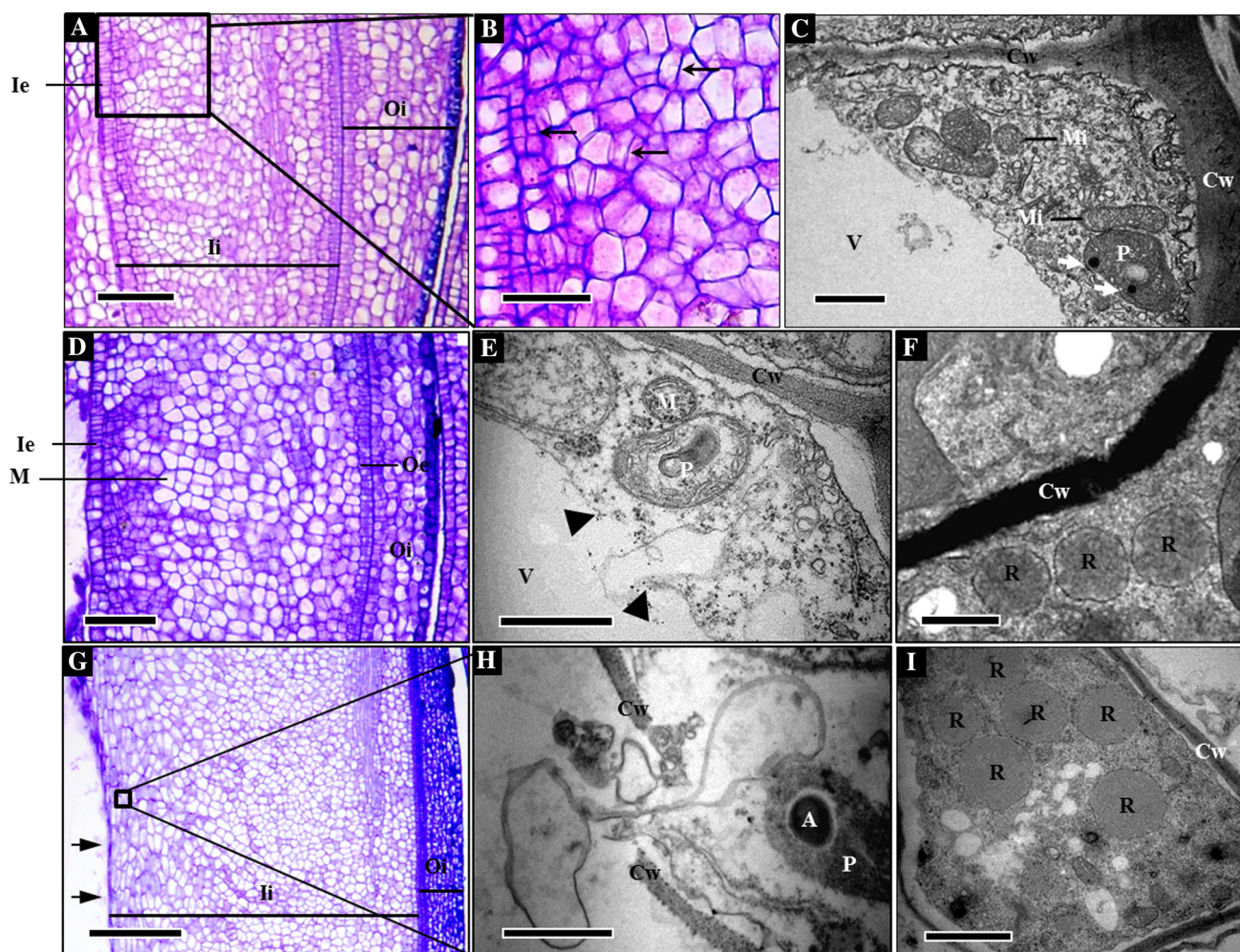
Fig. 4 Anatomy of the seed coat and ultrastructure of the inner integument of *J. curcas*. Light (**a**, **b**, **d**, **g**) and transmission electron microscopy (**c**, **e**, **f**, **h**, **i**) as observed in longitudinal sections. **a** Inner and outer integuments of the ovule. **b** Magnification of the square area in A showing pattern of cell division (*arrows*). **c** Ultrastructure of the inner integument mesophyll of the ovule. Note the presence of several plastids, plastoglobuli (*arrow*) and mitochondrion. **d** Seed coat development at 5 days after pollination (DAP). **e**, **f** Ultrastructure of a seed at 5 DAP showing tonoplast rupture (*arrowheads*) and ricinosomes, respectively. **g** Seed coat development at 10 DAP. Note lysis of the mesophyll cells near the free nuclei of the endosperm forming a dark stained cell layer. **h**, **i** Ultrastructure of the inner integument mesophyll cells undergoing lysis at 10 DAP. Note the cell wall breakdown and ricinosomes. *A* amyloplast, *Cw* cell wall, *Ie* inner epidermis, *Ii* inner integument, *Mi* mitochondrion, *Me* mesophyll, *Oe* outer epidermis, *Oi* outer integument, *P* plastid, *R* ricinosomes, *V* vacuole. *Bars* = 250 μm (**a**), 200 μm (**b**), 1 μm (**c**), 50 μm (**d**), 1 μm (**e**, **f**), 200 μm (**g**), 1 μm (**h**) and 2 μm (**i**)

derived organelles called ricinosomes (Fig. 4f). By 10 DAP the inner epidermis of the inner integument had been consumed, except for those cells that were in close proximity to the remainants of the nucellus (data not shown). The mesophyll cells located near the free nuclei of the endosperm become larger, flattened and underwent lysis, resulting in a darkly stained layer (Fig. 4g, see arrows). At this stage, cell wall breakdown was observed (Fig. 4h) and ricinosomes were more common (Fig. 4i).

By 25 DAP, cell lysis extended to the innermost cells of the mesophyll (Fig. 5A) and peroxisomes were observed (Fig. 5B, C). The peroxisomes in the layer of cells undergoing lysis were already dismantling (Fig. 5B) while the peroxisomes near the outermost layers of the mesophyll, adjacent to the outer epidermis, were intact (Fig. 5C). By 30 DAP, all mesophyll cells of the inner integument located between the vascular system and the endosperm were consumed while the cells between the vascular system and the outer epidermis persisted (Fig. 5D). At that point, the outer epidermal cells of the inner integument and both inner and outer epidermal cells of the outer integument became palisade-like (Fig. 5D). However, the outer epidermal cells of the inner integument are larger than the epidermal cells of the outer integument and sclerify earlier than the outer integument. In the mature seed, the seed coat is made up of the remnants of the inner integument (i.e. vascular tissue, collapsed mesophyll cells and sclerified outer epidermis) (Fig. 5E) and the sclerified outer integument.
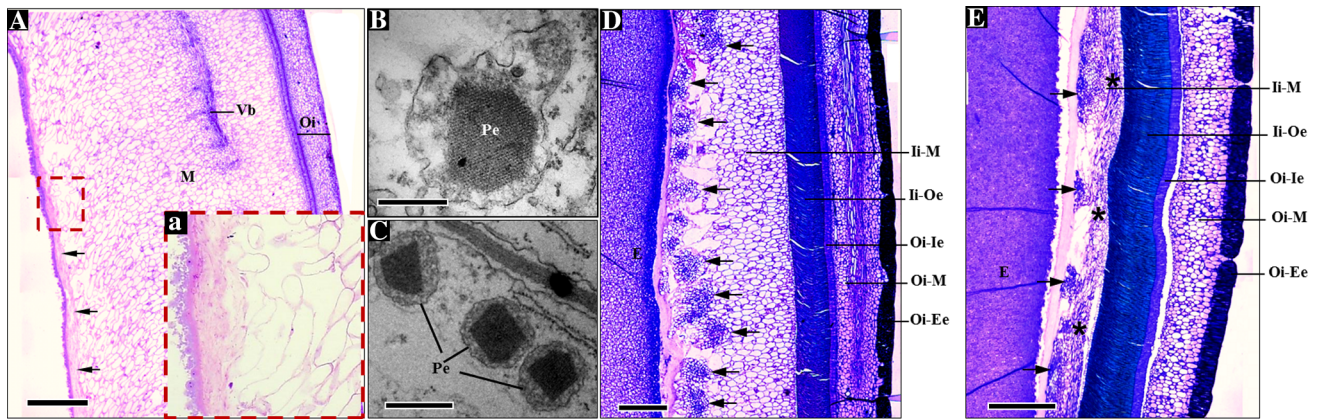
Fig. 5 Seed coat development of *J. curcas* under light (**A**, **D**, **E**) and transmission electron microscopy (**B**, **C**) as observed in longitudinal sections. **A** Seed coat at 25 DAP. Note detail of lysis in the innermost layers of the inner integument (*a*) and cell debris of the inner integument mesophyll (*arrows*). **B**, **C** Ultrastructure of the proximal and distal regions of the inner integument mesophyll at 25 DAP. Note the dismantling of peroxisomes in layer undergoing lysis (**B**) while the peroxisomes of the outermost layers of the mesophyll are intact (**C**). **D** Seed coat at 30 DAP. Note that the inner integument mesophyll cells are consumed up to the vascular bundles (*arrows*). **E** Seed coat at 35 DAP. Note the vascular bundles (*arrows*) and layers of compressed cells of the inner integument mesophyll (*asterisk*). *E* endosperm, *Ii-M* inner integument–mesophyll, *Ii-OE* inner integument–outer epidermis, *M* mesophyll, *Oi* outer integument, *Oi-Ee* outer integument–external epidermis, *Oi-Ii* outer integument–inner epidermis, *Oi-M* outer integument–mesophyll, *Pe* peroxisome, *Vb* vascular bundle. *Bars* 2 mm (**A**), 500 nm (**B**, **C**), 500 μm (**D**, **E**)
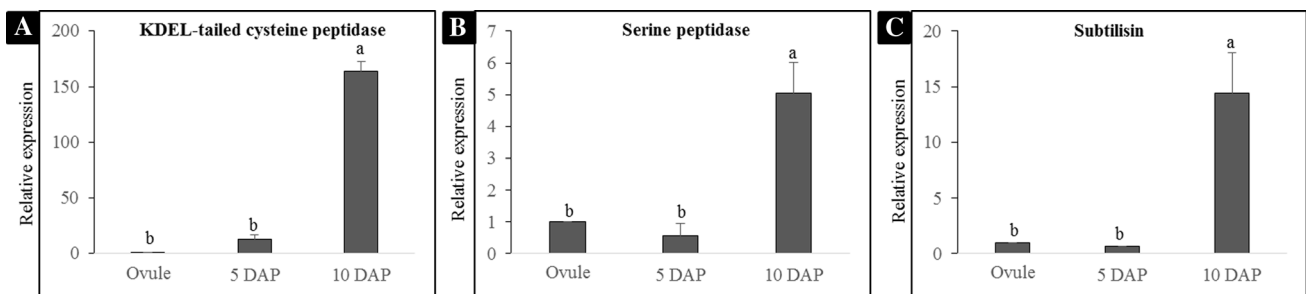

Fig. 6 Relative expression of genes coding to peptidases in the mesophyll of the inner integument of developing *J. curcas* seeds. **a** KDEL-tailed cysteine peptidase. **b** Serine peptidase. **c** Subtilisin. *DAP*, days after pollination. Statistical significance was determined through one-way analysis of variance (ANOVA) followed by Tukey's test ($\rho < 0.05$). *Distinct letters* indicate a significant difference

To ascertain the mechanisms underlying the extensive cell lysis observed in the inner integument, as well as the presence of ricinosomes that were observed during our ultrastructural analysis, we undertook a qPCR analysis of genes coding for three peptidases which are known to have a role in programmed cell death (PCD), namely a KDEL-tailed cysteine proteinase, a serine peptidase and a subtilisin. As shown in Fig. 6, transcripts for these genes reach maximum levels of expression at 10 DAP, thus suggesting that autolytic PCD likely functions in shaping seed development.

Discussion

In this report, we present novel anatomical and ultrastructural aspects on the development of *J. curcas* seeds. We also examined the role of PCD in shaping seed development. Additionally we identified root stomata at early times in development that may play a significant role in the absorption of water during early plant growth.

Although in *J. curcas* the zygote may be observed as early as at 2 DAP, it remains unchanged up to 10 DAP when the first cell divisions that originates the cells that will give rise to the embryo proper and suspensor takes place. The cotyledon embryo with its meristematic regions was observed only at 25 DAP, which is very slow if compared to *Ricinus communis* L. (Euphorbiaceae) where the first division is fast and the embryo rapidly differentiates before the endosperm becomes completely cellular (Singh 1954). On the other hand, *Euphorbia esula* L. (Euphorbiaceae) presents the same pattern of embryogenesis observed in *J. curcas* (Carmichael and Selbo 1999). Due to the rapid consumption of the nucellus, the maternal tissue closer to the developing embryo is the inner integument. This contrasts with *R. communis* that has a

long-lived and multiplicative nucellus close to the embryo (while the endosperm is coenocytic) and later in close contact with the cellularized endosperm until seed maturation, where it will be one of the tissue forming the mature seed coat (Greenwood and Bewley 1981).

In the developing seed, the suspensor is first seen at 15 DAP and remains functional up to 30 DAP where its demise correlates with the beginning of the maturation phase of the embryo proper. At early stages, the suspensor cells were highly vacuolated, which is in accordance with its role in the storage of water and other dissolved substances required for embryo development, as suggested by Kull and Arditti (2002).

The anatomical and ultrastructural analysis, along with the expression analysis of genes coding for peptidases, allow us to suggest the occurrence of two types of PCD during the differentiation of the seed coat of *J. curcas* (i.e. autolytic and non-autolytic PCD) according to the classification of van Doorn (2011). PCD of the inner integument occurred gradually, beginning from proximal end of the inner integument and moving to the distal region. This is in contrast to seed coat development of *Vigna unguiculata* (L.) Walp. that occurs from the outside layers of the seed to the inside layers (Lima et al. 2015). Cell layers between the vascular tissue and the developing endosperm (proximal region) disappear completely as observed by the anatomical analysis, while cell layers between the vascular tissue and the testa (distal region) persists in the mature seed as a layer of compressed cells. In the former region it was observed the tonoplast rupture followed by the rapid clearance of the cytoplasm. These features allow us to classify this PCD as autolytic. On the other hand, although we observed tonoplast rupture at the distal region there was not a rapid clearance of the cytoplasm that allows us to classify this PCD as the non-autolytic type. This reasoning is supported by a previous report (Soares et al. 2014) in which we showed that peptidases and carbohydrases have a higher expression level in the proximal region when compared with the distal region. Additionally, we have also demonstrated that plastid dismantling was faster at the proximal region (Shah et al. 2016), thus giving support to the hypothesis that the PCD occurring in the distal region of the inner integument is of the non-autolytic type, while that in the proximal region has the hallmarks of autolytic PCD.

To support the data observed in the ultrastructural analysis that PCD in the inner integument mesophyll is already occurring in early stages of development (up to 10 DAP) we evaluated the gene expression of cysteine and serine peptidases in the ovule and in developing seeds during early embryogenesis. All the peptidases evaluated were up-regulated indicating the progress of the PCD and supporting the observations of the anatomical and ultrastructural analysis. The KDEL-tailed cysteine peptidase that is recognized to be a hallmark of tissues undergoing PCD (Greenwood et al. 2005; Helm et al. 2008; Nogueira et al. 2012; Rocha et al. 2013; Zhou et al. 2016) had their highest level of expression coinciding with the highest number of ricinosomes. These organelles store inactive KDEL-tailed cysteine peptidases and were observed in several examples of plants in process of PCD (Schmid et al. 1999; Trobacher et al. 2013; Battelli et al. 2014). This result indicates that the presence of ricinosomes and the abundance of the KDEL-tailed cysteine peptidase transcript are positively correlated. Moreover, the fact that the serine peptidases were also up-regulated indicates that an array of peptidases must be involved in the PCD occurring at early developmental stages of *J. curcas* seed coat differentiation.

Certain anatomical features of *J. curcas* embryos, such as the presence of four seminal roots, stomata at the seminal root zone and developed protoxylem, are indicative of adaptation to a rapid absorption and transport of water. The presence of four seminal roots indicates a propensity to fast development of the root system, the presence of stomata facilitates water and minerals uptake during seedling emergence, while the occurrence of differentiated cells of protoxylem makes the water transport more efficient. These anatomical features may be crucial for the successful establishment of seedlings in dry environments. It may represent an adaptive strategy for the seeds of species which grow in arid or semiarid environments where rainfall is variable in time and space and occurs in pulses (Noy-Meir 1973; Flores and Briones 2001). Stomata in the root zone, particularly in embryos, are an unusual feature that is associated with gaseous exchange in the xeromorphic Mediterranean species *Ceratonia siliqua* L. (Christodoulakis et al. 2002). However, we understand that stomata in embryos may play a different role instead. The presence of stomata in the seminal root zone of *J. curcas* embryo may contribute to fast water uptake as showed by the assay of the apoplastic tracer Lucifer Yellow. To the best of our knowledge, it is the first time that water uptake by seminal root stomata were experimentally shown.

Although both articulated and non-articulated laticifers were reported in *J. curcas* (Rudall 1987), our study shows that all laticifers are articulated. The breakdown of the adjoining cell walls as well as anastomosing of rows is early in the seed embryo.

Conclusions

Our findings relate to the ontogeny of *J. curcas* seed development and provide insights regarding the types of PCD occurring in the inner integument. The nutrition of the

embryo proper and endosperm is provided by the inner integument and not by the nucellus which is short-lived, contrary to that of *R. communis* which remains alive until seed maturation. Finally, we suggest that the presence of four seminal roots, stomata at the seminal root zone and developed protoxylem, are indicative of adaptation to a fast absorption and transport of water.

Author contribution statement FAPC and AAS conceived and designed research. IACC, ELS, JRSN and MLBL performed the experiments and analyzed data. FAPC and ELS wrote the paper.

Compliance with ethical standards

Conflict of interest The authors declare that they have no conflict of interest.

References

Battelli R, Lombardi L, Picciarelli P et al (2014) Expression and localisation of a senescence-associated KDEL-cysteine protease from *Lilium longiflorum* tepals. Plant Sci 214:38–46. doi:10.1016/j.plantsci.2013.09.011

Carmichael JS, Selbo SM (1999) Ovule, embryo sac, embryo, and endosperm development in leafy spurge (*Euphorbia esula*). Can J Bot 77:599–610

Christodoulakis NS, Menti J, Galatis B (2002) Structure and development of stomata on the primary root of *Ceratonia siliqua* L. Ann Bot 89:23–29. doi:10.1093/aob/mcf002

Costa GGL, Cardoso KC, Del Bem LEV et al (2010) Transcriptome analysis of the oil-rich seed of the bioenergy crop *Jatropha curcas* L. BMC Genom 11:462. doi:10.1186/1471-2164-11-462

Flores J, Briones O (2001) Plant life-form and germination in a Mexican inter-tropical desert: effects of soil water potential and temperature. J Arid Environ 47:485–497. doi:10.1006/jare.2000.0728

Greenwood JS, Bewley JD (1981) Seed development in *Ricinus communis* (castor bean). I. Descriptive morphology. Can J Bot 60:1751–1760

Greenwood JS, Helm M, Gietl C (2005) Ricinosomes and endosperm transfer cell structure in programmed cell death of the nucellus during *Ricinus* seed development. Proc Natl Acad Sci USA 102:2238–2243. doi:10.1073/pnas.0409429102

Helm M, Schmid M, Hierl G et al (2008) KDEL-tailed cysteine endopeptidases involved in programmed cell death, intercalation of new cells, and dismantling of extensin scaffolds. Am J Bot 95:1049–1062. doi:10.3732/ajb.2007404

Hirakawa H, Tsuchimoto S, Sakai H et al (2012) Upgraded genomic information of *Jatropha curcas* L. Plant Biotechnol 29:123–130. doi:10.5511/plantbiotechnology.12.0515a

Junqueira CU (1990) O uso de cortes finos de tecidos na Medicina e Biologia. Meios e Métodos 66:167–171

Karnovsky MJJ (1965) A formaldehyde-glutaraldehyde fixative of high osmolality for use in electron microscopy. J Cell Biol 27:137–138

King AJ, Li Y, Graham IA (2011) Profiling the developing *Jatropha curcas* L. seed transcriptome by pyrosequencing. Bioenergy Res 4:211–221

Kull T, Arditti J (eds) (2002) Orchid biology: reviews and perspectives, vol 8. Springer

Laosatit K, Tanya P, Somta P et al (2016) De novo transcriptome analysis of apical meristem of *Jatropha* spp. Using 454 pyrosequencing platform, and identification of SNP and EST-SSR markers. Plant Mol Biol Rep 34:786–793. doi:10.1007/s11105-015-0961-z

Lima NB, Trindade FG, da Cunha M et al (2015) Programmed cell death during development of cowpea (*Vigna unguiculata* (L.) Walp.) seed coat. Plant Cell Environ 38:718–728. doi:10.1111/pce.12432

Liu H, Wang C, Komatsu S et al (2013) Proteomic analysis of the seed development in *Jatropha curcas*: from carbon flux to the lipid accumulation. J Proteom 91:23–40. doi:10.1016/j.jprot.2013.06.030

Livak KJ, Schmittgen TD (2001) Analysis of relative gene expression data using real-time quantitative PCR and the 2(−Delta DeltaC(T)) method. Methods 25:402–408. doi:10.1006/meth.2001.1262

Mardhiah HH, Ong HC, Masjuki HH et al (2017) A review on latest developments and future prospects of heterogeneous catalyst in biodiesel production from non-edible oils. Renew Sustain Energy Rev 67:1225–1236

Natarajan P, Parani M (2011) De novo assembly and transcriptome analysis of five major tissues of *Jatropha curcas* L. using GS FLX titanium platform of 454 pyrosequencing. BMC Genomics 12:191. doi:10.1186/1471-2164-12-191

Natarajan P, Kanagasabapathy D, Gunadayalan G et al (2010) Gene discovery from *Jatropha curcas* by sequencing of ESTs from normalized and full-length enriched cDNA library from developing seeds. BMC Genom 11:606. doi:10.1186/1471-2164-11-606

Nogueira FCS, Palmisano G, Soares EL et al (2012) Proteomic profile of the nucellus of castor bean (*Ricinus communis* L.) seeds during development. J Proteom 75:1933–1939. doi:10.1016/j.jprot.2012.01.002

Noy-Meir I (1973) Desert ecosystems: environment and producers. Annu Rev Ecol Syst 4:25–51. doi:10.1146/annurev.es.04.110173.000325

Oparka KJ, Prior DAM (1988) Movement of Lucifer Yellow CH in potato tuber storage tissues: a comparison of symplastic and apoplastic transport. Planta 176:533–540. doi:10.1007/BF00397661

Rocha AJ, Soares EL, Costa JH et al (2013) Differential expression of cysteine peptidase genes in the inner integument and endosperm of developing seeds of *Jatropha curcas* L. (Euphorbiaceae). Plant Sci. doi:10.1016/j.plantsci.2013.08.009

Rudall PJ (1987) Laticifers in Euphorbiaceae a conspectus. Bot J Linn Soc 94:143–163. doi:10.1111/j.1095-8339.1987.tb01043.x

Sato S, Hirakawa H, Isobe S et al (2011) Sequence analysis of the genome of an oil-bearing tree, *Jatropha curcas* L. DNA Res 18:65–76. doi:10.1093/dnares/dsq030

Schmid M, Simpson D, Gietl C (1999) Programmed cell death in castor bean endosperm is associated with the accumulation and release of a cysteine endopeptidase from ricinosomes. PNAS 96:14159–14164

Shah M, Soares EL, Carvalho PC et al (2015) Proteomic analysis of the endosperm ontogeny of *Jatropha curcas* L seeds. J Proteome Res. doi:10.1021/acs.jproteome.5b00106

Shah M, Soares EL, Lima MLB et al (2016) Deep proteome analysis of gerontoplasts from the inner integument of developing seeds of *Jatropha curcas*. J Proteom 143:346–352. doi:10.1016/j.jprot.2016.02.025

Singh RP (1954) Structure and development of seeds in Euphorbiaceae—*Ricinus communis* L. Phytomorphology 4:118–123

Singh RP (1970) Structure and development of seeds in Euphorbiaceae: *Jatropha* species. Beitr Biol Pflanz 47:79–90

Soares EL, Shah M, Soares AA et al (2014) Proteome analysis of the inner integument from developing *Jatropha curcas* L. seeds. J Proteome Res 13:3562–3570. doi:10.1021/pr5004505

Trobacher CP, Senatore A, Holley C, Greenwood JS (2013) Induction of a ricinosomal-protease and programmed cell death in tomato endosperm by gibberellic acid. Planta 237:665–679. doi:10.1007/s00425-012-1780-1

Van Doorn WG (2011) Classes of programmed cell death in plants, compared to those in animals. J Exp Bot 62:4749–4761. doi:10.1093/jxb/err196

Xu R, Wang R, Liu A (2011) Expression profiles of genes involved in fatty acid and triacylglycerol synthesis in developing seeds of *Jatropha* (*Jatropha curcas* L.). Biomass Bioenerg 35:1683–1692. doi:10.1016/j.biombioe.2011.01.001

Zhou LZ, Howing T, Muller B et al (2016) Expression analysis of KDEL-CysEPs programmed cell death markers during reproduction in *Arabidopsis*. Plant Reprod 29:265–272